Available online at www.sciencedirect.com
ScienceDirect
Phytochemistry 69 (2008) 772–782
PHYTOCHEMISTRY
www.elsevier.com/locate/phytochem

Diastereomeric stilbene glucoside dimers from the bark of Norway spruce (*Picea abies*)

Sheng-Hong Li [a], Xue-Mei Niu [a], Stefan Zahn [b], Jonathan Gershenzon [a,*], Jennie Weston [b], Bernd Schneider [a,*]

[a] *Max Planck Institute for Chemical Ecology, Beutenberg Campus, Hans-Knöll-Straße 8, D-07745 Jena, Germany*
[b] *Institute of Organic and Macromolecular Chemistry, Friedrich Schiller University, Humboldtstraße 10, D-07743 Jena, Germany*

Received 13 July 2007; received in revised form 29 August 2007
Available online 29 October 2007

Abstract

As part of a long-term study of the chemical defenses of Norway spruce (*Picea abies*) against herbivores and pathogens, a phytochemical survey of the phenolics in the bark was carried out. Eight stilbene glucoside dimers, designated as piceasides A–H (**1a**–**4b**), were isolated as four 1:1 mixtures of inseparable diastereomers. Their structures were determined by extensive spectroscopic means including 1D (^{1}H and ^{13}C) and 2D NMR (^{1}H–^{1}H COSY, HSQC, HMBC, ROESY) spectra, and were supported by enzymatic hydrolysis and computational analysis.

Keywords: Norway spruce; *Picea abies*; Bark; Stilbene glucoside dimers; Piceasides A–H; Diastereomers

1. Introduction

Norway spruce (*Picea abies* (L.) Karst.), a member of the pine family, is the most abundant conifer species in the boreal forests of Eurasia and has considerable ecological and economic importance. It has been frequently used as a model system to study the defense mechanisms of conifers against bark beetles and their associated fungi (Christiansen et al., 1999; Erbilgin et al., 2006; Franceschi et al., 2000, 2002, 2005; Hudgins et al., 2004; Krokene et al., 2001, 2003; Schmidt et al., 2005; Zeneli et al., 2006). Among spruce defenses, the terpenoid-containing oleoresin has been a frequent research topic (Martin et al., 2002, 2004; Schmidt et al., 2005; Viiri et al., 2001; Zeneli et al., 2006). However, the phenolics of this species have been much less studied, even though these substances may be almost as abundant as terpenes and also have a role in defense. One major reason is the structural diversity and complexity of Norway spruce phenolic substances, especially polyphenolics. To our knowledge, more than 60 phenolic compounds of various types have been isolated and identified from Norway spruce, including simple phenolic compounds, phenylpropanoids, stilbenes, lignans, flavonoids, procyanidins, etc. (Brignolas et al., 1995, 1998; Lieutier et al., 2003; Viiri et al., 2001; Zeneli et al., 2006). In order to get insight into the possible defensive function of phenolics present in Norway spruce bark, phytochemical investigations were carried on 70% aqueous acetone extracts from the whole bark. As a result, four pairs of new diastereomeric stilbene glucoside dimers, namely, piceasides A–G (**1ab**–**4ab**), were isolated and characterized.

2. Results and discussion

Compounds **1a** and **1b**, **3a** and **3b**, and **4a** and **4b** were isolated from the water-soluble fraction of a 70% aqueous acetone extract of lyophilized bark from 4-year-old sap-

* Corresponding authors. Tel.: +49 3641 571600; fax: +49 3641 571601 (B. Schneider), tel.: +49 3641 571300; fax: +49 3641 571302 (J. Gershenzon).
E-mail addresses: gershenzon@ice.mpg.de (J. Gershenzon), schneider@ice.mpg.de (B. Schneider).

0031-9422/$ - see front matter © 2007 Elsevier Ltd. All rights reserved.
doi:10.1016/j.phytochem.2007.08.033

lings. Work-up of the same fraction from the extract of the fresh bark of a 25 m-high tree yielded compounds **2a** and **2b** and **4a** and **4b** (for details, see Section 3). These compounds were obtained as pairs of 1:1 mixtures after separation by repeated open column chromatography and/or semi-preparative reversed-phase HPLC. Silica gel TLC of these mixtures developed with different combinations of solvent mixtures such as $CHCl_3$–MeOH–H_2O (3:2:0.5) showed highly homogenous spots. However, on analytical HPLC each of these mixtures displayed twin peaks which were only partially separated. Variation of the elution system did not improve the separation. Structure determinations were therefore carried out on the mixtures.

Compounds **1a** and **1b** were obtained as a dark brown amorphous solid. Positive ESI-TOF-MS showed $[M+Na]^+$ ion peaks at *m/z* 833.5 and negative ESI-TOF-MS showed $[M-H]^-$ at *m/z* 809.3, corresponding to a molecular weight of 810. A molecular formula of $C_{40}H_{42}O_{18}$ was determined for **1a** and **1b** through high resolution ESI-TOF-MS measurement of the ion at *m/z* 809 (*m/z* 809.2259, $[M-H]^-$, calcd: 809.2293). The ^1H NMR spectrum (Table 1) of **1a** and **1b** showed two sets of signals, which, at the same position, were either completely overlapped or partially overlapped with only a few signals being separated, suggesting that the structures of compounds **1a** and **1b** were very close to each other. The signals in the spectrum occurred basically in three regions (I: δ_H 7.0–6.0; II: δ_H 5.4–4.4; III: δ_H 4.0–3.3). Their coupling relationships were achieved through careful analysis of their coupling constants and the correlations in an ^1H–^1H COSY spectrum. The aromatic region (I) consisted of two partially overlapping ABC spin systems [**1a**: δ_H 6.827 (H-2″), 6.755 (H-5″), 6.689 (H-6″); **1b**: δ_H 6.824 (H-2″), 6.762 (H-5″), 6.696 (H-6″)] of 1,3,4-trisubstituted phenyl rings (ring A), two additional partially overlapping ABC spin systems [**1a**: δ_H 6.414 (H-10″), 6.482 (H-12″), 6.347 (H-14″); **1b**: δ_H 6.421 (H-10″), 6.482 (H-12″), 6.305 (H-14″)] of 1,3,5-trisubstitued phenyl rings (ring B), two completely overlapping ABC spin systems [**1a** and **1b**: δ_H 6.752 (H-10), 6.435 (H-12), 6.590 (H-14)] of 1,3,5-trisubstituted phenyl rings (ring D), two partially overlapping AM spin systems [**1a**: δ_H 6.944 (H-2), 6.697 (H-6); **1b**: δ_H 6.944 (H-2), 6.724 (H-6)] of 1,3,4,5-tetrasubstituted phenyl rings (ring C), and two partially overlapping olefinic proton systems [**1a**: δ_H 6.954 (H-7), 6.790 (H-8); **1b**: δ_H 6.961 (H-7), 6.796 (H-8)] of *trans*-substituted double bonds. Region II was constituted by two partially overlapping AX spin systems [**1a**: δ_H 5.370 (H-7″), 4.449 (H-8″); **1b**: δ_H 5.359 (H-7″), 4.455 (H-8″)] characteristic of dihydrobenzofuran moieties (Waffo-Teguo et al., 2001), and doublets at δ_H 4.884 (2H, H-1′ of **1a** and **1b**), 4.785 (H-1‴ of **1a**) and 4.869 (H-1‴ of **1b**) corresponding to four protons attached to anomeric C-1 of hexopyranoses. The latter, together with the observation of 24 dramatically overlapped protons in region III, indicated the existence of four β-glucosyl residues. The ^{13}C NMR and HSQC spectra demonstrated, in addition to resonances of the four glucosyl substituents (Table 1), four methines at δ_C 95.13 (*d*), 95.10 (*d*) and 59.36 (2C, *d*) arising from the dihydrobenzofuran moieties (Waffo-Teguo et al., 2001) and 52 carbons (26 methines and 26 quaternary carbons) in the aromatic region (δ_C 103–161). The magnetic nonequivalence of H-10 and H-14, and H-10″ and H-14″, revealed that the glucose moieties were ascribable to rings B and D, which was confirmed by the ^1H–^{13}C long-range correlations between the H-1′ and H-1‴ of the corresponding glucose and C-11 and C-11″ in the HMBC spectrum (Table 1). From these data, compounds **1a** and **1b** were deduced to be stilbene glucoside dimers consisting of two astringin units, connected through a dihydrofuran ring moiety, forming a skeleton similar to that of resveratrol (*E*)-dehydrodimer (Waffo-Teguo et al., 2001) and its analogs. This finding was not unexpected since astringin is a major stilbene glucoside present in the bark of Norway spruce (Mannila and Talvitie, 1992).

Initially, it was thought that **1a** differed from **1b** by interchanging the phenyl rings A and B on the dihydrobenzofuran moiety since two possible connections (C-7″–O–C–4/C-8″–C-5 and C-7″–C-5/C-8″–O-4) could occur. However, the HMBC spectrum (Table 1) displayed the same correlations for **1a** and **1b**, indicating that they should have the same planar structure. The coupling constants between H-7″ and H-8″ in **1a** and **1b** were 8.0 Hz and 8.5 Hz, respectively, suggesting a *trans* relative stereochemistry at the two chiral centers (C-7″ and C-8″) for both compounds, which was also consistent with the rOe correlations observed in the ROESY spectrum (Table 5). Another possibility was that we were dealing with a single compound displaying atropisomerism from a hindered rotation of ring A and the bulky glucosylated ring B. However, this could be excluded by variable-temperature ^1H NMR studies. ^1H NMR spectra measured between 7–50 °C in methanol-d_4 and 80 °C in DMSO-d_6 did not show any differences in the ratio between **1a** and **1b**, suggesting that the two isomers were not interchangeable. Therefore, the difference between **1a** and **1b** could only arise from their absolute stereochemistry at C-7″ and C-8″. The compound with a stereochemistry of 7″*R**, 8″*R** was designated **1a**, and that with the opposite stereochemistry, 7″*S**, 8″*S**, was designated **1b**. Upon enzymatic hydrolysis with cellulase, compounds **1a** and **1b** gave a racemic mixture of aglycones showing only one set of NMR signals. The lack of any CD absorption of the aglycones further supported the conclusion that compounds **1a** and **1b** are a pair of diastereomeric astringin dimers (Fig. 1), which were named piceasides A and B, respectively.

The mixture of compounds **2a** and **2b** was obtained as a pale brown amorphous solid, with a molecular formula of $C_{41}H_{44}O_{18}$ based on the positive ion ESI-TOF-MS peak at *m/z* 847.5 $[M+Na]^+$ and the negative ion ESI-TOF-MS peak at *m/z* 823.4 $[M-H]^-$, as confirmed by the high resolution ESI-TOF-MS (*m/z* 823.2403, $[M-H]^-$, calcd: 823.2449). The ^1H and ^{13}C NMR spectra closely resembled those of **1a** and **1b** (Tables 1 and 2), with the only difference being the presence of two additional methoxyl groups [δ_H

Table 1
^{1}H and ^{13}C NMR data and ^{1}H–^{13}C long-range correlations of **1a** and **1b** in CD_3OD

Position	δ_H (**1a**)[a]	δ_C (**1a**)[b]	δ_H (**1b**)[a]	δ_C (**1b**)[b]	HMBC (**1a** and **1b**)[c]
1		133.07 (*s*)		133.07 (*s*)	
2	6.944 (*br s*)	115.16 (*d*)	6.944 (*br s*)	115.09 (*d*)	C-3, 4, 6, 7, 8
3		142.49 (*s*)		142.49 (*s*)	
4		148.72 (*s*)		148.72 (*s*)	
5		133.10 (*s*)		133.02 (*s*)	
6	6.697 (*overlap*)	115.93 (*d*)	6.724 (*br s*)	115.98 (*d*)	C-2, 4, 5, 7
7	6.954 (*d*, 16.5)	130.23 (*d*)	6.961 (*d*, 16.5)	130.19 (*d*)	C-2, 6, 8, 9
8	6.790 (*d*, 16.5)	127.24 (*d*)	6.796 (*d*, 16.5)	127.21 (*d*)	C-1, 7, 9, 10, 14
9		141.30 (*s*)		141.30 (*s*)	
10	6.752 (*overlap*)	107.12 (*d*)	6.752 (*overlap*)	107.05 (*d*)	C-8, 11, 12, 14
11		160.46 (*s*)		160.46 (*s*)	
12	6.435 (*dd*, 2.0, 2.1)	104.23 (*d*)	6.435 (*dd*, 2.0, 2.1)	104.23 (*d*)	C-10, 11, 13, 14
13		159.58 (*s*)		159.58 (*s*)	
14	6.590 (*dd*, 1.7, 2.0)	108.36 (*d*)	6.590 (*dd*, 1.7, 2.0)	108.36 (*d*)	C-8, 10, 12, 13
1′	4.884 (*d*, 7.5)	102.36 (*d*)	4.884 (*d*, 7.5)	102.36 (*d*)	C-11, 3′, 5′
2′	3.32–3.50 (*overlap*)	74.97 (*d*)	3.32–3.50 (*overlap*)	74.97 (*d*)	
3′	3.32–3.50 (*overlap*)	78.03 (*d*)	3.32–3.50 (*overlap*)	78.03 (*d*)	
4′	3.32–3.50 (*overlap*)	71.50 (*d*)	3.32–3.50 (*overlap*)	71.49 (*d*)	
5′	3.32–3.50 (*overlap*)	78.19 (*d*)	3.32–3.50 (*overlap*)	78.20 (*d*)	
6′	3.912 (*br d*, 12.0)	62.61 (*t*)	3.912 (*br d*, 12.0)	62.61 (*t*)	C-4′, 5′
	3.699 (*dd*, 6.0, 12.0)		3.699 (*dd*, 6.0, 12.0)		
1″		133.59 (*s*)		133.53 (*s*)	
2″	6.827 (*d*, 2.0)	114.22 (*d*)	6.824 (*d*, 2.0)	114.34 (*d*)	C-3″, 4″, 6″, 7″
3″		146.48 (*s*)		146.50 (*s*)	
4″		146.64 (*s*)		146.64 (*s*)	
5″	6.755 (*d*, 8.0)	116.29 (*d*)	6.762 (*d*, 8.0)	116.29 (*d*)	C-1″, 3″, 4″
6″	6.689 (*dd*, 2.0, 8.0)	119.04 (*d*)	6.696 (*dd*, 2.0, 8.0)	119.16 (*d*)	C-2″, 4″, 7″
7″	5.370 (*d*, 8.0)	95.13 (*d*)	5.359 (*d*, 8.5)	95.10 (*d*)	C-4, 5, 1″, 2″, 6″, 8″, 9″
8″	4.449 (*d*, 8.0)	59.36 (*d*)	4.455 (*d*, 8.5)	59.36 (*d*)	C-4, 5, 6, 1″, 7″, 9″, 10″, 14″
9″		145.73 (*s*)		145.50 (*s*)	
10″	6.414 (*dd*, 1.7, 1.9)	109.00 (*d*)	6.421 (*dd*, 1.7, 1.8)	108.73 (*d*)	C-8″, 11″, 12″, 14″
11″		160.52 (*s*)		160.40 (*s*)	
12″	6.482 (*dd*, 2.1, 2.2)	103.88 (*d*)	6.482 (*dd*, 2.1, 2.2)	103.64 (*d*)	C-10″, 11″, 13″, 14″
13″		159.86 (*s*)		159.89 (*s*)	
14″	6.347 (*dd*, 1.6, 1.7)	110.21 (*d*)	6.305 (*dd*, 1.6, 1.8)	110.32 (*d*)	C-8″, 10″, 12″, 13″
1‴	4.785 (*d*, 7.0)	102.29 (*d*)	4.869 (*d*, 7.5)	101.82 (*d*)	C-11″, 3‴, 5‴
2‴	3.32–3.50 (*overlap*)	74.81 (*d*)	3.32–3.50 (*overlap*)	74.86 (*d*)	
3‴	3.32–3.50 (*overlap*)	77.92 (*d*)	3.32–3.50 (*overlap*)	77.95 (*d*)	
4‴	3.32–3.50 (*overlap*)	71.18 (*d*)	3.32–3.50 (*overlap*)	71.04 (*d*)	
5‴	3.32–3.50 (*overlap*)	77.96 (*d*)	3.32–3.50 (*overlap*)	77.02 (*d*)	
6‴	3.803 (*dd*, 2.0, 12.0)	62.23 (*t*)	3.828 (*dd*, 2.0, 12.0)	62.33 (*t*)	C-4‴, 5‴
	3.699 (*overlap*)		3.699 (*overlap*)		

[a] ^{1}H NMR chemical shifts followed by multiplicities and coupling constants in parentheses. Chemical shifts are given relative to TMS which was used as a reference. Coupling constants *J* are in Hz. Spectra were measured at 500 MHz. Signals of **1a** and **1b** at the same position might be interchangeable.
[b] ^{13}C NMR chemical shifts followed by multiplicities. Chemical shifts are given relative to TMS which was used as a reference. Spectra were measured at 125 MHz. Signals of **1a** and **1b** at the same position might be interchangeable.
[c] ^{1}H–^{13}C Long-range correlations (from H to C) observed in the HMBC spectrum.

3.817, 3.824 and δ_C 56.49 (2C)]. Considering that the bark of Norway spruce contains yet another major stilbene glucoside, isorhapontin (Mannila and Talvitie, 1992), which is actually 3-O-methylated astringin, the methoxyl group in compounds **2a** and **2b** is very likely located at either the C-3 or the C-3″ position. Comparison of the NMR data of **2a** and **2b** with those of **1a** and **1b** revealed that the chemical shifts of C-3 and its surrounding carbons and protons in **2a** and **2b** remained almost unchanged, whereas the signals for C-3″ and the surrounding carbons and protons shifted significantly, implying the location of the additional methoxyl groups at C-3″. This was confirmed by the presence of ^{1}H–^{13}C long-range correlations between the methoxyl protons and C-3″ for both **2a** and **2b** in HMBC experiments. It was therefore deduced that compounds **2a** and **2b** are a pair of diastereomeric stilbene dimers formed between astringin and isorhapontin, and were named piceasides C and D, respectively (Fig. 1).

A mixture of compounds **3a** and **3b** was obtained as a brown sticky solid having the same molecular formula ($C_{41}H_{44}O_{18}$) as **2a** and **2b**, as deduced from positive ESI-TOF-MS (*m*/*z* 847.5, $[M+Na]^+$) and negative ESI-TOF-MS (*m*/*z* 823.2, $[M-H]^-$). This was verified by high resolution ESI-TOF-MS (*m*/*z*: 823.2402, $[M-H]^-$, calcd:

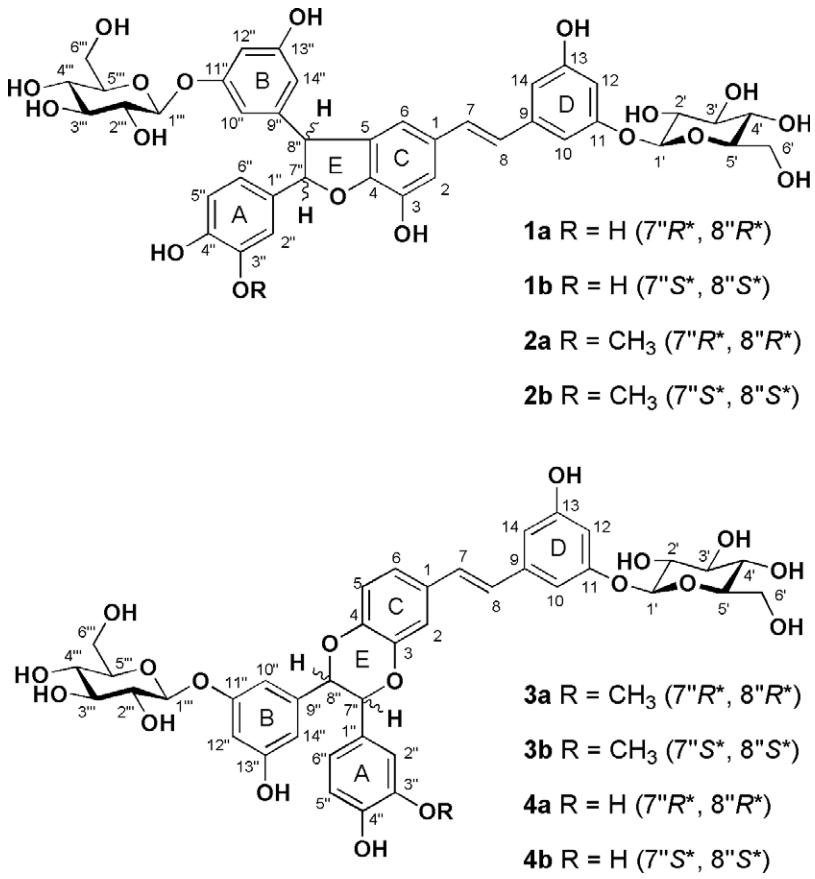

Fig. 1. Chemical structures of piceasides A (**1a**), B (**1b**), C (**2a**), D (**2b**), E (**3a**), F (**3b**), G (**4a**) and H (**4b**).

823.2449). The ^{1}H NMR (Table 3) and ^{1}H–^{1}H COSY spectra exhibited two separated and two partially overlapping ABC spin systems due to the presence of 1,3,4-trisubstituted phenyl rings (rings A and C), two separated and two completely overlapping ABC spin systems originating from 1,3,5-trisubstituted phenyl rings (rings B and D), two partially overlapping olefinic proton systems with large coupling constants ($J = 16.3$ and 16.1 Hz) diagnostic of two *trans*-substituted double bonds, two pairs of AB doublets between δ_H 4.74–4.85, four glucose moieties and a methoxyl group. Most of these signals were also observed in the ^{1}H NMR spectra of the above two pairs of compounds, suggesting that compounds **3a** and **3b** were again a pair of related diastereomeric stilbene glucoside dimers. The major difference between this pair and the above two pairs can be attributed to the structures of rings C and E, in which a 1,3,4,5-tetrasubstituted phenyl ring (AM spin system) and a dihydrofuran ring (AX spin system) in **1a**–**2b** were replaced, respectively by a 1,3,4-trisubstituted phenyl ring (ABC spin system) and a dihydro-1,4-dioxin ring (AB spin system) in **3a** and **3b**. The characterization of ring E in **3a** and **3b** as a dihydro-1,4-dioxin was based mainly on the dramatic downfield shift of H-8″/C-8″ (from *ca.* $\delta_{H/C}$ 4.5/59 in **1ab**–**2ab** to *ca.* $\delta_{H/C}$ 4.8/82 in **3ab**) and the upfield shift of H-7″/C-7″ (from *ca.* $\delta_{H/C}$ 5.4/95 in **1ab**–**2ab** to *ca.* $\delta_{H/C}$ 4.8/82 in **3ab**). Thus compounds **3a** and **3b** were identified as another type of stilbene glucoside dimers in Norway spruce, having the same skeleton as cassigarols E and F (Baba et al., 1994), two stilbene dimers which were identified from *Cassia garrettiana* after acetylation.

Determination of the connections between the two stilbene units in this particular type of compound is not trivial. The use of routine HMBC experiments, as indicated in the literature (Baba et al., 1994), is problematic due to the inherent difficulty in obtaining definitive correlations from H-7″ and H-8″ through the oxygen bridge to C-3 and C-4. Biosynthetic considerations are sometimes invoked for elucidating such structures, but this could lead to ambiguous structures like maackin-*cis* from *Maackia amurensis* (Kulesh et al., 1999) and maackin from *Caragana rosea* (Yang et al., 2005). These compounds are probably identical with cassigarol F and its *trans*-isomer cassigarol E (Baba et al., 1994), respectively, since no details were reported on how their two structural units were connected. Recently, a Constant Time-HMBC method (Xiang et al., 2005) was applied for the structure determination of cassigarols E and G, and the decisive correlations were successfully achieved. To detect the HMBC correlations between H-7″ and C-3 and between H-8″ and C-4 of compounds **3a** and **3b**, it was sufficient in our hands to set the digital resolution (time domain) in the ^{13}C dimension to 256 or

Table 2
^{1}H and ^{13}C NMR data and ^{1}H–^{13}C long-range correlations of **2a** and **2b**

Position	δ_H (**2a**)[a]	δ_C (**2a**)[b]	δ_H (**2b**)[a]	δ_C (**2b**)[b]	HMBC (**2a** and **2b**)[c]
1		133.11 (*s*)		133.15 (*s*)	
2	6.947 (*br s*)	115.25 (*d*)	6.950 (*br s*)	115.18 (*d*)	C-4, 6, 7, 8
3		142.54 (*s*)		142.54 (*s*)	
4		148.69 (*s*)		148.69 (*s*)	
5		133.22 (*s*)		133.19 (*s*)	
6	6.695 (*br s*)	115.96 (*d*)	6.718 (*br s*)	115.91 (*d*)	C-2, 4, 5, 7
7	6.952 (*d*, 16.0)	130.23 (*d*)	6.956 (*d*, 16.0)	130.20 (*d*)	C-2, 6, 8, 9
8	6.780 (*d*, 16.0)	127.34 (*d*)	6.795 (*d*, 16.0)	127.30 (*d*)	C-1, 7, 9, 10, 14
9		141.30 (*s*)		141.31 (*s*)	
10	6.745 (*dd*, 1.6, 1.9)	107.10 (*d*)	6.748 (*dd*, 1.6, 2.0)	107.16 (*d*)	C-8, 11, 12, 14
11		160.48 (*s*)		160.48 (s)	
12	6.431 (*dd*, 2.0, 2.1)	104.29 (*d*)	6.431 (*dd*, 2.0, 2.1)	104.29 (*d*)	C-10, 11, 13, 14
13		159.61 (*s*)		159.61 (*s*)	
14	6.587 (*dd*, 1.6, 1.7)	108.41 (*d*)	6.587 (*dd*, 1.6, 1.7)	108.41 (*d*)	C-8, 10, 12, 13
1′	4.489 (*d*, 7.4)	102.39 (*d*)	4.489 (*d*, 7.4)	102.39 (*d*)	C-11, 3′, 5′
2′	3.31–3.49 (*overlap*)	75.00 (*d*)	3.31–3.49 (*overlap*)	75.00 (*d*)	
3′	3.31–3.49 (*overlap*)	78.07 (*d*)	3.31–3.49 (*overlap*)	78.07 (*d*)	
4′	3.31–3.49 (*overlap*)	71.55 (*d*)	3.31–3.49 (*overlap*)	71.53 (*d*)	
5′	3.31–3.49 (*overlap*)	78.23 (*d*)	3.31–3.49 (*overlap*)	78.23 (*d*)	
6′	3.908 (*br d*, 12.0)	62.64 (*t*)	3.908 (*br d*, 12.0)	62.64 (*t*)	C-4′, 5′
	3.693 (*dd*, 5.8, 12.0)		3.693 (*dd*, 5.8, 12.0)		
1″		133.29 (*s*)		133.31 (*s*)	
2″	6.943 (*d*, 1.8)	110.81 (*d*)	6.954 (*d*, 1.9)	110.91 (*d*)	C-3″, 4″, 6″, 7″
3″		149.16 (*s*)		149.16 (*s*)	
4″		147.85 (*s*)		147.87 (*s*)	
5″	6.781 (*d*, 7.9)	116.21 (*d*)	6.786 (*d*, 8.0)	116.21 (*d*)	C-1″, 3″, 4″
6″	6.800 (*overlap*)	120.25 (*d*)	6.805 (*overlap*)	120.38 (*d*)	C-2″, 4″, 7″
7″	5.434 (*d*, 8.5)	95.21 (*d*)	5.428 (*d*, 8.5)	95.16 (*d*)	C-4, 5, 1″, 2″, 6″, 8″, 9″
8″	4.480 (*d*, 8.5)	59.39 (*d*)	4.487 (*d*, 8.5)	59.37 (*d*)	C-4, 5, 6, 1″, 7″, 9″, 10″, 14″
9″		145.47 (*s*)		145.28 (*s*)	
10″	6.419 (*dd*, 1.6, 2.1)	109.09 (*d*)	6.431 (*overlap*)	108.90 (*d*)	C-8″, 11″, 12″, 14″
11″		160.55 (*s*)		160.46 (*s*)	
12″	6.490 (*dd*, 2.1, 2.2)	103.95 (*d*)	6.492 (*dd*, 2.1, 2.2)	103.72 (*d*)	C-10″, 11″, 13″, 14″
13″		159.91 (*s*)		159.92 (*s*)	
14″	6.351 (*dd*, 1.6, 1.9)	110.40 (*d*)	6.313 (*dd*, 1.6, 1.9)	110.51 (*d*)	C-8″, 10″, 12″, 13″
1‴	4.796 (*d*, 7.4)	102.29 (*d*)	4.869 (*d*, 7.3)	101.92 (*d*)	C-11″, 3‴, 5‴
2‴	3.31–3.49 (*overlap*)	74.88 (*d*)	3.31–3.49 (*overlap*)	74.84 (*d*)	
3‴	3.31–3.49 (*overlap*)	77.98 (*d*)	3.31–3.49 (*overlap*)	77.95 (*d*)	
4‴	3.31–3.49 (*overlap*)	71.06 (*d*)	3.31–3.49 (*overlap*)	71.24 (*d*)	
5‴	3.31–3.49 (*overlap*)	78.09 (*d*)	3.31–3.49 (*overlap*)	78.01 (*d*)	
6‴	3.787 (*dd*, 2.3, 12.1)	62.25 (*t*)	3.822 (*dd*, 2.3, 12.0)	62.38 (*t*)	C-4‴, 5‴
	3.688 (*overlap*)		3.688 (*overlap*)		
OCH_3	3.817 (3H, *q*)	56.49 (*q*)	3.824 (3H, *q*)	56.49 (*q*)	C-3″

[a] ^{1}H NMR chemical shifts followed by multiplicities and coupling constants in parentheses. Chemical shifts are given relative to TMS which was used as a reference. Coupling constants *J* are in Hz. Spectra were measured at 500 MHz. Signals of **2a** and **2b** at the same position might be interchangeable.
[b] ^{13}C NMR chemical shifts followed by multiplicities. Chemical shifts are given relative to TMS which was used as a reference. Spectra were measured at 125 MHz. Signals of **2a** and **2b** at the same position might be interchangeable.
[c] ^{1}H–^{13}C Long-range correlations (from H to C) observed in the HMBC spectrum.

512 K data points and enhance sensitivity by using a cryogenically cooled probe and a long measuring time. The observed cross peaks (Fig. 2) unequivocally indicated the presence of C-7″–O–C–3 and C-8″–O–C–4 linkages. The assignment of the glucose units to rings B and D, and the methoxyl groups to C-3″ were based on HMBC correlations between the protons at the anomeric centres and C-11 and C-11″, and between the methyl protons and C-3″, respectively. Furthermore, these assignments were consistent with the chemical shifts of related signals in the ^{1}H and ^{13}C NMR spectra (Table 3). The *trans* configuration at C-7″ and C-8″ in **3a** and **3b** was established from the coupling constant between H-7″ and H-8″ ($J = 8.1$ Hz) and the ROESY correlations observed (Table 5). Variable-temperature ^{1}H NMR studies (7–50 °C in methanol-d_4 and 80 °C in DMSO-d_6) suggested that these two isomers, like **1ab** and **2ab**, are not interchangeable, i.e. are not rotational isomers. Similarly, enzymatic hydrolysis of **3a** and **3b** led to a racemic mixture of new aglycones with only one set of NMR signals and no CD absorption, similar to the properties of the aglycones formed from **1a** and **1b**. Compounds **3a** and **3b** were accordingly characterized as another pair of

Table 3
^{1}H and ^{13}C NMR data and ^{1}H–^{13}C long-range correlations of **3a** and **3b**

Position	δ_H (**3a**)[a]	δ_C (**3a**)[b]	δ_H (**3b**)[a]	δ_C (**3b**)[b]	HMBC (**3a** and **3b**)[c]
1		132.66 (*s*)		132.63 (*s*)	
2	7.176 (*d*, 2.0)	115.95 (*d*)	7.168 (*d*, 2.0)	115.95 (*d*)	C-1, 3, 4, 6, 7
3		145.47 (*s*)		145.47 (*s*)	
4		145.04 (*s*)		145.11 (*s*)	
5	6.966 (*d*, 8.4)	118.26 (*d*)	6.948 (*d*, 8.4)	118.23 (*d*)	C-1, 3, 4, 6
6	7.092 (*dd*, 2.0, 8.4)	121.31 (*d*)	7.081 (*dd*, 2.0, 8.4)	121.31 (*d*)	C-2, 4, 7
7	7.027 (*d*, 16.3)	129.64 (*d*)	7.024 (*d*, 16.0)	129.64 (*d*)	C-1, 2, 6, 8, 9
8	6.904 (*d*, 16.3)	128.18 (*d*)	6.908 (*d*, 16.0)	128.18 (*d*)	C-1, 7, 9, 10, 14
9		141.15 (*s*)		141.15 (*s*)	
10	6.811 (*overlap*)	107.23 (*d*)	6.808 (*overlap*)	107.23 (*d*)	C-8, 11, 12, 14
11		160.51 (*s*)		160.51 (*s*)	
12	6.469 (*dd*, 1.8, 2.2)	104.43 (*d*)	6.468 (*dd*, 1.7, 2.3)	104.43 (*d*)	C-10, 11, 13, 14
13		159.65 (*s*)		159.65 (*s*)	
14	6.638 (*overlap*)	108.57 (*d*)	6.637 (*overlap*)	108.57 (*d*)	C-8, 10, 12, 13
1′	4.900 (*d*, 7.4)	102.43 (*d*)	4.900 (*d*, 7.4)	102.13 (*d*)	C-11, 3′, 5′
2′	3.26–3.50 (*overlap*)	74.99 (*d*)	3.26–3.50 (*overlap*)	74.99 (*d*)	
3′	3.26–3.50 (*overlap*)	78.07 (*d*)	3.26–3.50 (*overlap*)	78.07 (*d*)	
4′	3.26–3.50 (*overlap*)	71.52 (*d*)	3.26–3.50 (*overlap*)	71.52 (*d*)	
5′	3.26–3.50 (*overlap*)	78.26 (*d*)	3.26–3.50 (*overlap*)	78.26 (*d*)	
6′	3.931 (*d*, 12.0)	62.62 (*t*)	3.926 (*d*, 12.0)	62.62 (*t*)	C-4′, 5′
	3.711 (*dd*, 5.9, 12.0)		3.711 (*dd*, 5.9, 12.0)		C-4′, 5′
1″		129.33 (*s*)		129.19 (*s*)	
2″	6.688 (*d*, 2.0)	112.47 (*d*)	6.660 (*d*, 1.8)	112.47 (*d*)	C-1″, 3″, 4″, 6″, 7″
3″		148.72 (*s*)		148.72 (*s*)	
4″		147.86 (*s*)		147.86 (*s*)	
5″	6.704 (*d*, 8.2)	115.86 (*d*)	6.688 (*d*, 8.4)	115.85 (*d*)	C-1″, 3″, 4″, 6″
6″	6.596 (*dd*, 2.0, 8.2)	121.88 (*d*)	6.641 (*dd*, 1.8, 8.4)	121.77 (*d*)	C-2″, 4″, 7″
7″	4.756 (*d*, 8.1)	82.02 (*d*)	4.839 (*d*, 8.1)	81.74 (*d*)	C-3, 1″, 2″, 6″, 8″, 9″
8″	4.797 (*d*, 8.1)	82.22 (*d*)	4.797 (*d*, 8.1)	82.21 (*d*)	C-4, 1″, 7″, 9″, 10″, 14″
9″		140.14 (*s*)		140.26 (*s*)	
10″	6.182 (*dd*, 1.6, 1.8)	108.44 (*d*)	6.462 (*dd*, 1.6, 1.9)	109.06 (*d*)	C-8″, 11″, 12″, 14″
11″		159.94 (*s*)		160.08 (*s*)	
12″	6.437 (*dd*, 2.2, 2.3)	105.27 (*d*)	6.477 (*dd*, 2.2, 2.3)	105.56 (*d*)	C-10″, 11″, 13″, 14″
13″		159.33 (*s*)		159.36 (*s*)	
14″	6.407 (*dd*, 1.6, 2.1)	109.70 (*d*)	6.241 (*dd*, 1.6, 1.8)	110.53 (*d*)	C-8″, 10″, 12″, 13″
1‴	4.439 (*d*, 7.7)	102.64 (*d*)	4.751 (*d*, 7.7)	102.68 (*d*)	C-11″, 5‴
2‴	3.26–3.50 (*overlap*)	74.87 (*d*)	3.26–3.50 (*overlap*)	74.82 (*d*)	
3‴	3.26–3.50 (*overlap*)	77.93 (*d*)	3.26–3.50 (*overlap*)	77.83 (*d*)	
4‴	3.26–3.50 (*overlap*)	71.41 (*d*)	3.26–3.50 (*overlap*)	71.23 (*d*)	
5‴	3.26–3.50 (*overlap*)	78.02 (*d*)	3.26–3.50 (*overlap*)	77.97 (*d*)	
6‴	3.853 (*br d*, 12.2)	62.53 (*t*)	3.849 (*br d*, 12.0)	62.42 (*t*)	C-4‴, 5‴
	3.670 (*dd*, 5.5, 12.2)		3.709 (*overlap*)		C-4‴, 5‴
OCH_3	3.724 (3H, *s*)	56.54 (*q*)	3.741 (3H, *s*)	56.51 (*q*)	C-3″

[a] ^{1}H NMR chemical shifts followed by multiplicities and coupling constants in parentheses. Chemical shifts are given relative to TMS which was used as a reference. Coupling constants *J* are in Hz. Spectra were measured at 500 MHz. Signals of **3a** and **3b** at the same position might be interchangeable.
[b] ^{13}C NMR chemical shifts followed by multiplicities. Chemical shifts are given relative to TMS which was used as a reference. Spectra were measured at 125 MHz. Signals of **3a** and **3b** at the same position might be interchangeable.
[c] ^{1}H–^{13}C Long-range correlations (from H to C) observed in the HMBC spectrum.

diastereomeric stilbene dimers constituted from astringin and isorhapontin units, and named piceasides E and F, respectively (Fig. 1).

The mixture of compounds **4a** and **4b** was isolated as a pale brown amorphous solid, and their molecular formula of $C_{40}H_{42}O_{18}$ (identical to that of **1a** and **1b**) was established by positive ESI-TOF-MS (*m*/*z* 833.5, $[M + Na]^+$) and negative ESI-TOF-MS (*m*/*z* 809.3, $[M-H]^-$), and confirmed by high resolution ESI-TOF-MS (*m*/*z*: 809.2256, $[M-H]^-$, 809.2293). Inspection of their 1D (^{1}H and ^{13}C) and 2D (^{1}H–^{1}H COSY, HSQC and HMBC) NMR data (Table 4) suggests that the basic skeleton of **4a** and **4b** is the same as that of **3a** and **3b**. The only difference between the two pairs of compounds was the missing 3″-*O*-methyl group. Hence compounds **4a** and **4b** were concluded to again be a pair of diastereomeric astringin dimers, and named piceasides G and H, respectively (Fig. 1).

In previous work, monomeric stilbene glucosides, especially astringin and isorhapontin, were found to be predominant phenolics in the bark of Norway spruce (Mannila and Talvitie, 1992). While the bark was also proposed to contain stilbene polymers (Tisler and Muck,

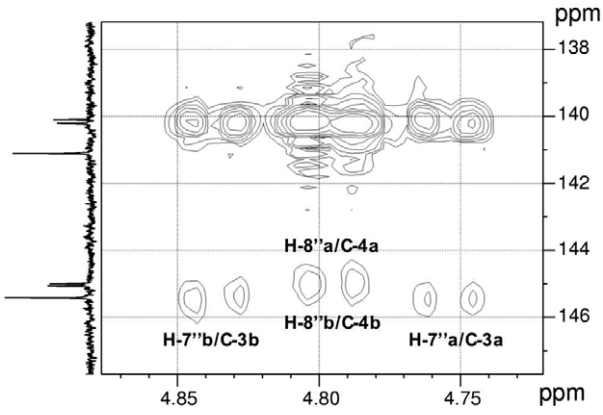

Fig. 2. Partial HMBC spectrum of compounds **3a** and **3b** showing the correlations between the two structural units (Sample concentration: 6 mg/ml; TD: F2 = 4 k, F1 = 256; NS = 104).

1999), none of these compounds were isolated and characterized until this report.

Comparing the optical activity of other stilbene dimers, maackin A, a dihydrofuran-type stilbene dimer whose structure is identical with the aglycone of **1a** or **1b**, was isolated as an optically active compound [CD (*c* 4.0, MeOH): $[\theta]_{260} = +920$ (br)] (Kulesh et al., 1999). Its *cis*-isomer (maackin A-*cis*) showed also CD absorption (CD (*c* 4.0, MeOH): $[\theta]_{248} = +1300$) (Kulesh et al., 1999). Another similar stilbene dimer, resveratrol (*E*)-dehydrodimer, which bears two hydroxyl substituents less than maackin A at rings A and C, was also reported to be optically active but with rather small optical rotation values, $[\alpha]_D^{20} - 1.7$ (*c* 0.23, MeOH) (Cichewicz et al., 2000) and $[\alpha]_D^{20} - 1.15$ (*c* 7.3, acetone) (Waffo-Teguo et al., 2001). Parvifolol D, having an additional *O*-methyl group attached to 3-OH of the aglycone of **2a** or **2b**, showed $[\alpha]_D + 7$ (*c* 0.11, MeOH) (Tanaka et al., 2001). Scirpusin B, a ε-type stilbene dimer also containing a dihydrofuran ring, was optically inactive (Baba et al., 1994) whereas its *cis*-isomer, scirpusin B-*cis* showed a CD effect (CD (*c* 4.0, MeOH): $[\theta]_{260} = -1047$) (Kulesh et al., 1999). A dihydro-1,4-dioxin-type stilbene dimer, cassigarol E, having the same structure as the aglycone of **4a** and **4b**, was optically inactive (Baba et al., 1994). However, the two structures, maackin and maackin-*cis*, which might be cassigarol E and its *cis*-isomer cassigarol F, were reported to have $[\alpha]_D^{20} - 57.0$ (*c* 0.40, MeOH) (Yang et al., 2005) and CD (*c* 4.0, MeOH): $[\theta]_{220} = +74$, $[\theta]_{250} = -831$ (Kulesh et al., 1999), respectively. Obviously some of these values are not convincing due to their small optical rotation values or are contradictory and therefore may need to be reinvestigated. An interesting biomimic transformation of resveratrol with peroxidases and thallium (III) nitrate was shown to result in a high yield (68%) of the dimer, (±)-ε-viniferin (Takaya et al., 2005). All of the above evidence suggest that some stilbene dimers of both the dihydrofuran-type and dihydro-1,4-dioxin-types exist as racemates in plants, which could well explain why the stilbene glucoside dimers from Norway spruce were all obtained as pairs of diastereomers.

In order to shed more light on these interesting structures, two pairs of compounds (**1a** and **1b**, **4a** and **4b**) were selected for density functional calculations at the TPSS(RI)/def2-SVP level of theory; a relatively high level of theory which essentially ensures thermodynamical accuracy. In order to employ this level of theory, it proved necessary to simplify the structures somewhat. All four structures share the same flexible "tail" which is quite remote from the centers of interest (7″, 8″). The steric "stiffness" of the planar E/C ring ensures that this tail cannot undergo specific interactions with the possible diasteromeric region. This allows for simplification of the structures by eliminating the "tail" (cutting it off between C-1 and C-7) without significantly affecting the *relative* energies of the substructures of interest. Four new partial structures **1a′**, **1b′** and **4a′**, **4b** were generated in this manner and fully optimized at the TPSS(RI)/def2-SVP level of theory. All four are viable conformational minima and can thus be expected to be experimentally present. The small energy differences between the pairs of structures ($\Delta E_{\mathbf{1a',1b'}} = 1.8$ kJ/mol and $\Delta E_{\mathbf{4a',4b'}} = 3.4$ kJ/mol) clearly reinforces the view that these compounds share a diasteromeric relationship. The energy difference is slightly smaller for the **1a′**, **1b′** pair due to the presence of a stabilizing intramolecular hydrogen bond between 6‴-OH and 3-OH which is not present in either **4a′** or **4b′**. It is quite interesting that the relative energies calculated for compounds **1a/b** and **4a/b** is with 31.8 kJ/mol ($\Delta E_{\mathbf{1a',4a'}}$) and 26.6 kJ/mol ($\Delta E_{\mathbf{1b',4b'}}$) an entire magnitude of order larger. This indicates that the dihydrofuran type stilbene dimers are thermodynamically considerably more stable than the dihydro-1,4-dioxin-type dimers. This may be the reason why most stilbene dimers isolated from the plants contain a dihydrofuran ring whereas only a few possess a dihydro-1,4-dioxin moiety.

The existence of stilbene glucoside dimers in Norway spruce raises questions about their biosynthesis. Since, as in the monomeric stilbene glucosides astringin and isorhapontin, glucosyl moieties are attached regiospecifically to one of the hydroxyl groups of the acetogenic aryl but not the phenylpropanoid-derived ring, one could speculate that glucosidation occurs prior to rather than after dimerization. Dimerization after conjugation is also more reasonable because the monomer glucosides are abundant in Norway spruce bark while the monomer aglycones occur only in trace amounts. It has been suggested that peroxidases and dirigent proteins might be involved in the dimerization of resveratrol to ε-viniferin and δ-viniferin (Pezet et al., 2004). Interestingly, a family of dirigent proteins and dirigent protein-like genes associated with wound- and insect induced defense response was recently identified in Sitka spruce (*Picea sitchensis*) (Ralph et al., 2006). Further work is needed to understand more about the biosynthesis of stilbene dimers and their functions in the plant.

Table 4
^{1}H and ^{13}C NMR data and ^{1}H–^{13}C long-range correlations of **4a** and **4b**

Position	δ_H (**4a**)[a]	δ_C (**4a**)[b]	δ_H (**4b**)[a]	δ_C (**4b**)[b]	HMBC (**4a** and **4b**)[c]
1		132.55 (*s*)		132.51 (*s*)	
2	7.164 (*d*, 2.0)	115.76 (*d*)	7.153 (*d*, 2.0)	115.76 (*d*)	C-1, 3, 4, 6, 7
3		145.41 (*s*)		145.41 (*s*)	
4		144.92 (*s*)		145.01 (*s*)	
5	6.968 (*d*, 8.4)	118.17 (*d*)	6.943 (*d*, 8.4)	118.13 (*d*)	C-1, 3, 4, 6
6	7.092 (*dd*, 2.0, 8.4)	121.19 (*d*)	7.082 (*dd*, 2.0, 8.4)	121.19 (*d*)	C-2, 4, 7
7	7.033 (*d*, 16.3)	129.60 (*d*)	7.028 (*d*, 16.1)	129.60 (*d*)	C-1, 2, 6, 8, 9
8	6.909 (*d*, 16.3)	128.09 (*d*)	6.915 (*d*, 16.1)	128.07 (*d*)	C-1, 7, 9, 10, 14
9		141.09 (*s*)		141.09 (*s*)	
10	6.810 (*dd*, 1.6, 1.7)	107.18 (*d*)	6.814 (*dd*, 1.5, 1.7)	107.18 (*d*)	C-8, 11, 12, 14
11		160.42 (*s*)		160.42 (*s*)	
12	6.463 (*overlap*)	104.35 (*d*)	6.463 (*overlap*)	104.35 (*d*)	C-10, 11, 13, 14
13		159.55 (*s*)		159.55 (*s*)	
14	6.634 (*overlap*)	108.49 (*d*)	6.634 (*overlap*)	108.49 (*d*)	C-8, 10, 12, 13
1′	4.897 (*d*, 7.1)	102.34 (*d*)	4.897 (*d*, 7.1)	102.34 (*d*)	C-11, 3′, 5′
2′	3.28–3.49 (*overlap*)	74.92 (*d*)	3.28–3.49 (*overlap*)	74.92 (*d*)	
3′	3.28–3.49 (*overlap*)	77.98 (*d*)	3.28–3.49 (*overlap*)	77.98 (*d*)	
4′	3.28–3.49 (*overlap*)	71.43 (*d*)	3.28–3.49 (*overlap*)	71.43 (*d*)	
5′	3.28–3.49 (*overlap*)	78.17 (*d*)	3.28–3.49 (*overlap*)	78.17 (*d*)	
6′	3.930 (*dd*, 2.2, 12.1)	62.54 (*t*)	3.930 (*dd*, 2.2, 12.1)	62.54 (*t*)	C-4′, 5′
	3.709 (*dd*, 6.0, 12.1)		3.709 (*dd*, 6.0, 12.1)		C-4′, 5′
1″		129.44 (*s*)		129.27 (*s*)	
2″	6.691 (*d*, 2.1)	115.87 (*d*)	6.663 (*d*, 2.0)	115.87 (*d*)	C-1″, 3″, 4″, 6″, 7″
3″		146.10 (*s*)		146.09 (*s*)	
4″		146.69 (*s*)		146.63 (*s*)	
5″	6.654 (*d*, 8.1)	116.02 (*d*)	6.641 (*d*, 8.2)	116.02 (*d*)	C-1″, 3″, 4″, 6″
6″	6.417 (*dd*, 2.1, 8.1)	121.05 (*d*)	6.483 (*dd*, 2.0, 8.2)	120.81 (*d*)	C-2″, 4″, 5″, 7″
7″	4.676 (*d*, 8.0)	81.96 (*d*)	4.773 (*d*, 8.0)	81.63 (*d*)	C-3, 1″, 2″, 6″, 8″, 9″
8″	4.803 (*d*, 8.0)	82.00 (*d*)	4.811 (*d*, 8.0)	81.94 (*d*)	C-1″, 7″, 9″, 10″, 14″
9″		140.07 (*s*)		140.21 (*s*)	
10″	6.165 (*dd*, 1.7, 1.8)	108.45 (*d*)	6.466 (*overlap*)	108.97 (*d*)	C-8″, 11″, 12″, 14″
11″		159.77 (*s*)		159.91 (*s*)	
12″	6.414 (*dd*, 2.1, 2.2)	105.22 (*d*)	6.457 (*dd*, 2.1, 2.2)	105.46 (*d*)	C-10″, 11″, 13″, 14″
13″		159.17 (*s*)		159.15 (*s*)	
14″	6.439 (*dd*, 1.6, 1.8)	109.40 (*d*)	6.261 (*dd*, 1.6, 1.8)	110.36 (*d*)	C-8″, 10″, 12″, 13″
1‴	4.414 (*d*, 7.7)	102.61 (*d*)	4.753 (*d*, 7.6)	102.54 (*d*)	C-11″, 5‴
2‴	3.28–3.49 (*overlap*)	74.80 (*d*)	3.28–3.49 (*overlap*)	74.76 (*d*)	
3‴	3.28–3.49 (*overlap*)	77.74 (*d*)	3.28–3.49 (*overlap*)	77.75 (*d*)	
4‴	3.28–3.49 (*overlap*)	71.18 (*d*)	3.28–3.49 (*overlap*)	71.25 (*d*)	
5‴	3.28–3.49 (*overlap*)	77.86 (*d*)	3.28–3.49 (*overlap*)	77.93 (*d*)	
6‴	3.861 (*dd*, 2.0, 12.1)	62.39 (*t*)	3.869 (*dd*, 1.8, 11.7)	62.36 (*t*)	C-4‴, 5‴
	3.691 (*dd*, 4.9, 12.1)		3.714 (*dd*, 4.7, 11.7)		C-4‴, 5‴

[a] ^{1}H NMR chemical shifts followed by multiplicities and coupling constants in parentheses. Chemical shifts are given relative to TMS which was used as a reference. Coupling constants *J* are in Hz. Spectra were measured at 500 MHz. Signals of **4a** and **4b** at the same position might be interchangeable.
[b] ^{13}C NMR chemical shifts followed by multiplicities. Chemical shifts are given relative to TMS which was used as a reference. Spectra were measured at 125 MHz. Signals of **4a** and **4b** at the same position might be interchangeable.
[c] ^{1}H–^{13}C Long-range correlations (from H to C) observed in the HMBC spectrum.

3. Experimental

3.1. General experimental procedures

^{1}H and 2D NMR (COSY, HSQC, HMBC, ROESY) experiments were performed on a Bruker Avance 500 NMR spectrometer equipped with a cryogenic TXI probehead. ^{13}C NMR experiments were carried out on a Bruker DRX 500 NMR spectrometer. ESI-TOF-MS and HR ESI-TOF-MS were run on a Quattro triple quadrupole mass spectrometer. IR spectra were recorded on a Bruker IFS55 spectrometer with KBr pellets. UV spectral data were taken on a Varian UV–Vis Cary spectrophotometer. Optical rotations were measured on a Propol Digital Automatic Polarimeter. CD measurements were realized on a Jasco J-810 spectropolarimeter. Column chromatography was performed either on Sephadex LH-20 (Amersham Biosciences AB, Uppsala, Sweden) or on MCI gel (70–150 μm, Mitsubishi Chemical Corporation, Tokyo, Japan). Fractions were monitored by TLC on silica gel and spots were visualized under UV light (254 nm) first, and then by heating plates sprayed with 10% H_2SO_4 in EtOH. Semipreparative reversed-phase HPLC isolations were performed on a Merck-Hitachi HPLC system composed of a L-4250 UV–

Table 5
Selected ROESY correlations of piceasides A and B (**1a** and **1b**) and piceasides E and F (**3a** and **3b**)

Proton	**1a** and **1b**	**3a** and **3b**
H-2	H-7	H-7, 8
H-6	H-14″	
H-7	H-2, 14	H-2, 14
H-8	H-14	H-2, 14
H-10	H-1′	H-1′
H-14	H-7, 8	H-7, 8
H-1′	H-10	H-10
H-2″	H-8″	H-8″, OCH_3
H-6″	H-8″	H-8″
H-7″	H-10″, 14″	H-10″, 14″
H-8″	H-2″, 6″	H-2″, 6″
H-10″	H-7″, 1‴	H-7″, 1‴
H-14″	H-6, 7″	H-7″
H-1‴	H-10″	H-10″

Vis detector and a L-6200A Intelligent Pump. The purifications were completed on a LiChrospher column (250×10 mm, 10 μm, LichroCART®, Germany) with flow rate of 3.0 mL/min and detection at 254 nm. All solvents used were of analytical or HPLC grade (Merck, Darmstadt, Germany).

3.2. Plant material

Two samples of Norway spruce (*Picea abies* (L.) Kars. Pinaceae) bark were used in this study. One was harvested from four 4-year-old saplings (clone 3369 Schongau) growing outdoors at the Max Planck Institute for Chemical Ecology (Jena, Germany) in October 2004. These were originally obtained from Samenklenge und Pflanzgarten (Laufen, Germany) in November 2003. The other sample was harvested from a randomly selected tree (approximately 25 m high) growing near Jena in January 2005.

3.3. Extraction and isolation

The bark of four saplings was peeled off with a blade, frozen immediately in liquid nitrogen, and lyophilized to give 150 g of dry material. A 100 g portion was ground into small pieces in a mortar with liquid nitrogen, and exhaustively extracted with 70% aqueous acetone (4×800 ml) by maceration at room temperature. The extracts were combined and evaporated *in vacuo* at 35 °C to remove the organic solvent and further concentrated to *ca.* 300 ml at the same temperature. Sequential partitioning with *n*-hexane, $CHCl_3$ and EtOAc (4×400 ml each) and evaporation to dryness afforded four extracts: an *n*-hexane extract (1.9 g), a $CHCl_3$ extract (0.9 g), an EtOAc extract (3.3 g), and an aqueous phase (27.0 g). The aqueous phase was subjected to column chromatography on a Sephadex LH-20 column eluted with H_2O, EtOH and 70% aqueous Me_2CO to give three fractions W1–W3. Fraction W3 (eluted with 70% aqueous Me_2CO) was further chromatographed on an MCI gel column with a MeOH/H_2O gradient (0%, 30%, 50%, 70%, 100%) to give five subfractions A–E. The eluent of subfraction B (30% MeOH) was again chromatographed on MCI gel eluting with a gradient of MeOH/H_2O (20%, 30%, 40%, 50%, 100%). A crude sample mainly containing **1a** and **1b** was obtained from the 40% MeOH eluate, which was further purified on a Sephadex LH-20 column with MeOH as eluent to yield **1a** and **1b** (10 mg). The eluent of subfraction C (50% MeOH) was separated by repeated semipreparative HPLC (A: H_2O, B: MeCN; 0–10 min: isocratic 20%B, 10–20 min: linear gradient of 20–30% of B, 20–30 min: linear gradient of 30–40% of B) to give **4a** and **4b** (15 mg) with R_t of 21.0 min. Similarly, compounds **3a** and **3b** (12 mg) were furnished from subfraction D with R_t of 13.94 min by using the same mobile phases but different gradients (0–10 min: isocratic 20%B, 10–17 min: linear gradient of 20–26% of B).

The bark (50 g) of the large tree was harvested with a blade at *ca.* 1.5 m above the ground, chopped into small slices and frozen immediately in liquid nitrogen. The frozen sample was milled directly without lyophilization, and then steeped in 70% aqueous acetone (500 ml) and exhaustively extracted as described above. The extracts were combined and partially evaporated *in vacuo* at 35 °C to remove acetone and gave a milky aqueous suspension, which was partitioned with EtOAc to remove lipophilic substances. The water-soluble part was directly subjected to column chromatography on MCI gel (300 g) eluting with a gradient of MeOH/H_2O (0%–15%–30%–50%–100%) to result in five fractions I–V. Fraction III (30% MeOH) was again chromatographed on MCI gel (100 g) with 25% → 30% → 35% → 40% → 50% MeOH in H_2O as eluents to provide crude compounds **2a** and **2b** (in 35% MeOH eluate), which was further purified on a Sephadex LH-20 column (100 g) with MeOH as eluent to yield **2a** and **2b** (6 mg). In a similar way, 10 mg of compounds **4a** and **4b** was also obtained from fraction IV (50% MeOH).

3.4. Piceasides A and B (*1a* and *1b*)

Dark brown amorphous solid; $[\alpha]_D^{24.9} - 35.6°$ ($c = 0.153$, CH_3OH); UV (CH_3OH) λ_{max} ($\log\varepsilon$): 203 (4.4), 331 (3.8) nm; IR ν_{max} (KBr): 3265, 2924, 2840, 1598, 1505, 1447, 1337, 1287, 1171, 1073, 1013 cm^{-1}; ^1H NMR (CD_3OD, 500 MHz) and ^{13}C NMR (CD_3OD, 125 MHz): see Table 1; Positive ESI-TOF-MS, *m/z* (rel. int.): 833.5 $[M+Na]^+$ (49); Negative ESI-TOF-MS, *m/z* (rel. int.): 809.3 $[M-H]^-$ (100); HR ESI-TOF-MS, *m/z*: 809.2259 (calcd. for $C_{40}H_{41}O_{18}$, 809.2293).

3.5. Enzymatic hydrolysis of *1a* and *1b*

In a 1 ml Eppendorf tube, 0.9 mg of compounds **1a** and **1b** were dissolved in 0.5 ml of McIlvain buffer (pH ≈ 3) which was prepared by mixing 75 ml of citric acid solution (21.008 g $C_6H_8O_7 \cdot H_2O$ in 1000 ml H_2O) with 25 ml of Na_2HPO_4 solution (35.62 g in 1000 ml H_2O). Cellulase (2 mg) was suspended in the above solution and incubated with a Thermomixer at 37 °C and 1400 rpm for 24 h. The

reaction mixture was extracted with 4×0.5 ml of EtOAc and dried with a stream of nitrogen to give 0.61 mg of aglycone. Aglycone of piceasides A and B: brown amorphous solid; ^{1}H NMR (CD_3OD, 500 MHz): δ_H 6.92 (1H, *d*, $J = 1.5$ Hz, H-2), 6.89 (1H, *d*, $J = 16.2$ Hz, H-7), 6.81 (1H, *d*, $J = 2.0$ Hz, H-2″), 6.75 (1H, *d*, $J = 8.1$ Hz, H-5″), 6.73 (1H, *d*, $J = 16.2$ Hz, H-8), 6.69 (1H, *dd*, $J = 2.0$, 8.1 Hz, H-6″), 6.68 (1H, overlap, H-6), 6.41 (2H, *d*, $J = 2.2$ Hz, H-10 and H-14), 6.17 (1H, *t*, $J = 2.2$ Hz, H-12″), 6.13 (2H, *d*, $J = 2.2$ Hz, H-10″ and H-14″), 6.13 (1H, *t*, $J = 2.2$ Hz, H-12), 5.34 (1H, *d*, $J = 8.2$ Hz, H-7″), 4.37 (1H, *d*, $J = 8.2$ Hz, H-8″); CD: no absorption.

3.6. Piceasides C and D (**2a** and **2b**)

Pale brown amorphous solid; $[\alpha]_D^{25.0} - 55.4°$ ($c = 0.108$, CH_3OH); UV (CH_3OH) λ_{max} ($\log\varepsilon$): 204 (4.5), 329 (3.9) nm; IR ν_{max} (KBr): 3274, 2924, 1594, 1514, 1448, 1335, 1272, 1221, 1161, 1125, 1068, 1017, 962, 813, 746, 657 cm^{-1}; ^{1}H NMR (CD_3OD, 500 MHz) and ^{13}C NMR (CD_3OD, 125 MHz): see Table 2; Positive ESI-TOF-MS, *m*/*z* (rel. int.): 847.5 $[M+Na]^+$ (30); Negative ESI-TOF-MS, *m*/*z* (rel. int.): 823.4 $[M-H]^-$ (100); HR ESI-TOF-MS, *m*/*z*: 823.2403 (calcd. for $C_{41}H_{43}O_{18}$, 823.2449).

3.7. Piceasides E and F (**3a** and **3b**)

Brown sticky solid; $[\alpha]_D^{24.9} - 41.9°$ ($c = 0.156$, CH_3OH); UV (CH_3OH) λ_{max} ($\log\varepsilon$): 202 (4.3), 323 (3.9) nm; IR ν_{max} (KBr): 3294, 2923, 1596, 1505, 1455, 1340, 1269, 1169, 1121, 1074, 1022, 824, 765, 687 cm^{-1}; ^{1}H NMR (CD_3OD, 500 MHz) and ^{13}C NMR (CD_3OD, 125 MHz): see Table 3; Positive ESI-TOF-MS, *m*/*z* (rel. int.): 847.5 $[M+Na]^+$ (100); Negative ESI-TOF-MS, *m*/*z* (rel. int.): 823.2 $[M-H]^-$ (100); HR ESI-TOF-MS, *m*/*z*: 823.2402 (calcd. for $C_{41}H_{43}O_{18}$, 823.2449).

3.8. Enzymatic hydrolysis of **3a** and **3b**

In a similar way to **1a** and **1b**, 0.7 mg of **3a** and **3b** was enzymatically hydrolyzed with cellulase to give 0.45 mg of aglycone. Aglycone of piceasides E and F: brown amorphous solid; ^{1}H NMR (CD_3OD, 500 MHz): δ_H 7.17 (1H, *d*, $J = 1.9$ Hz, H-2), 7.08 (1H, *dd*, $J = 1.9$, 8.4 Hz, H-6), 6.97 (1H, *d*, $J = 16.2$ Hz, H-7), 6.96 (1H, *d*, $J = 8.4$ Hz, H-5), 6.87 (1H, *d*, $J = 16.2$ Hz, H-8), 6.69 (1H, *d*, $J = 8.0$ Hz, H-5″), 6.65 (1H, *dd*, $J = 1.7$, 8.0 Hz, H-6″), 6.63 (1H, *d*, $J = 1.7$ Hz, H-2″), 6.46 (2H, *d*, $J = 2.1$ Hz, H-10 and H-14), 6.17 (1H, *t*, $J = 2.1$ Hz, H-12), 6.16 (1H, *t*, $J = 2.2$ Hz, H-12″), 6.09 (2H, *d*, $J = 2.2$ Hz, H-10″ and H-14″), 4.81 (1H, *d*, $J = 7.9$ Hz, H-7″), 4.72 (1H, *d*, $J = 7.9$ Hz, H-8″), 3.72 (3H, *s*, 3″-OCH_3); CD: no absorption.

3.9. Piceasides G and H (**4a** and **4b**)

Pale brown amorphous solid; $[\alpha]_D^{24.9} - 51.6°$ ($c = 0.118$, CH_3OH); UV (CH_3OH) λ_{max} ($\log\varepsilon$): 202 (4.3), 323 (3.9) nm; IR ν_{max} (KBr): 3321, 2924, 1601, 1506, 1454, 1339, 1270, 1166, 1117, 1070, 1042, 1018, 822, 682, 659 cm^{-1}; ^{1}H NMR (CD_3OD, 500 MHz) and ^{13}C NMR (CD_3OD, 125 MHz): see Table 4; Positive ESI-TOF-MS, *m*/*z* (rel. int.): 833.5 $[M+Na]^+$ (87); Negative ESI-TOF-MS, *m*/*z* (rel. int.): 809.3 $[M-H]^-$ (100); HR ESI-TOF-MS, *m*/*z*: 809.2256 (calcd. for $C_{40}H_{41}O_{18}$, 809.2293).

3.10. Quantum chemical methodology

The program package ORCA (http://www.thch.uni-bonn.de/tc/orca) was used for all calculations which were performed employing the TPSS (Tao et al., 2003) density functional in combination with the def2-SVP basis set (Weigend and Ahlrichs, 2005). The resolution of identity (RI) approximation (Eichkorn et al., 1995, 1997) was used for all calculations.

Acknowledgements

We thank A. Schmidt for providing the young spruce trees, I. Sattler for helping get the IR, UV and ORD data, and S. Bartram for CD measurements on the aglycones. This work was supported by a research fellowship from Alexander-von-Humboldt Foundation to S.-H. Li and funds from the Max Planck Society.

References

Baba, K., Kido, T., Taniguchi, M., Kozawa, M., 1994. Stilbenoids from *Cassia garrettiana*. Phytochemistry 36, 1509–1513.

Brignolas, F., Lacroix, B., Lieutier, F., Sauvard, D., Drouet, A., Claudot, A.-C., Yart, A., Berryman, A.A., Christiansen, E., 1995. Induced responses in phenolic metabolism in two Norway spruce clones after wounding and inoculations *with Ophiostoma polonicum*, a bark beetle-associated fungus. Plant Physiol. 109, 821–827.

Brignolas, F., Lieutier, F., Sauvard, D., Christiansen, E., Berryman, A.A., 1998. Phenolic predictors for Norway spruce resistance to the bark beetle *Ips typographus* (Coleoptera: Scolytidae) and an associated fungus, *Ceratocystis polonica*. Can. J. Forest Res. 28, 720–728.

Christiansen, E., Krokene, P., Berryman, A.A., Franceschi, V.R., Krekling, T., Lieutier, F., Lonneborg, A., Solheim, H., 1999. Mechanical injury and fungal infection induce acquired resistance in Norway spruce. Tree Physiol. 19, 399–403.

Cichewicz, R.H., Kouzi, S.A., Hamann, M.T., 2000. Dimerization of resveratrol by the grapevine pathogen *Botrytis cinerea*. J. Nat. Prod. 63, 29–33.

Eichkorn, K., Treutler, O., Öhm, H., Häser, M., Ahlrichs, R., 1995. Auxiliary basis-sets to approximate Coulomb potentials. Chem. Phys. Lett. 240, 283–289.

Eichkorn, K., Weigend, F., Treutler, O., Ahlrichs, R., 1997. Auxiliary basis sets for main row atoms and transition metals and their use to approximate Coulomb potentials. Theor. Chem. Acc. 97, 119–124.

Erbilgin, N., Krokene, P., Christiansen, E., Zeneli, G., Gershenzon, J., 2006. Exogenous application of methyl jasmonate elicits defenses in Norway spruce (*Picea abies*) and reduces host colonization by the bark beetle *Ips typographus*. Oecologia 148, 426–436.

Franceschi, V.R., Krokene, P., Krekling, T., Christiansen, E., 2000. Phloem parenchyma cells are involved in local and distant defense

responses to fungal inoculation or bark-beetle attack in Norway spruce (Pinaceae). Am. J. Bot. 87, 314–326.

Franceschi, V.R., Krekling, T., Christiansen, E., 2002. Application of methyl jasmonate on *Picea abies* (Pinaceae) stems induces defense-related responses in phloem and xylem. Am. J. Bot. 89, 578–586.

Franceschi, V.R., Krokene, P., Christiansen, E., Krekling, T., 2005. Anatomical and chemical defenses of conifer bark against bark beetles and other pests. New Phytol. 167, 353–375.

Hudgins, J.W., Christiansen, E., Franceschi, V.R., 2004. Induction of anatomically based defense responses in stems of diverse conifers by methyl jasmonate: a phylogenetic perspective. Tree Physiol. 24, 251–264.

Krokene, P., Solheim, H., Christiansen, E., 2001. Induction of disease resistance in Norway spruce (*Picea abies*) by necrotizing fungi. Plant Pathol. 50, 230–233.

Krokene, P., Solheim, H., Krekling, T., Christiansen, E., 2003. Inducible anatomical defense responses in Norway spruce stems and their possible role in induced resistance. Tree Physiol. 23, 191–197.

Kulesh, N.I., Maksimov, O.B., Fedoreev, S.A., Denisenko, V.A., Glasunov, V.P., Pokushalova, T.V., Glebko, L.I., 1999. About native components of extracts from *Maackia amurensis* wood. Chem. Nat. Compd. 35, 575–579.

Lieutier, F., Brignolas, F., Sauvard, D., Yart, A., Galet, C., Brunet, M., van de Sype, H., 2003. Intra- and inter-provenance variability in phloem phenols of *Picea abies* and relationship to a bark beetle-associated fungus. Tree Physiol. 23, 247–256.

Mannila, E., Talvitie, A., 1992. Stilbenes from *Picea abies* bark. Phytochemistry 31, 3288–3289.

Martin, D., Tholl, D., Gershenzon, J., Bohlmann, J., 2002. Methyl jasmonate induces traumatic resin ducts, terpenoid resin biosynthesis, and terpenoid accumulation in developing xylem of Norway spruce stems. Plant Physiol. 129, 1003–1018.

Martin, D.M., Faldt, J., Bohlmann, J., 2004. Functional characterization of nine Norway spruce TPS genes and evolution of gymnosperm terpene synthases of the TPS-d subfamily. Plant Physiol. 135, 1908–1927.

Pezet, R., Gindro, K., Viret, O., Spring, J.L., 2004. Glycosylation and oxidative dimerization of resveratrol are respectively associated to sensitivity and resistance of grapevine cultivars to downy mildew. Physiol. Mol. Plant Pathol. 65, 297–303.

Ralph, S., Park, J.Y., Bohlmann, J., Mansfield, S.D., 2006. Dirigent proteins in conifer defense: gene discovery, phylogeny, and differential wound- and insect-induced expression of a family of DIR and DIR-like genes in spruce (*Picea* spp.). Plant Mol. Biol. 60, 21–40.

Schmidt, A.Z.G., Hietala, A.M., Fossdal, C.G., Krokene, P., Christiansen, E., Gershenzon, J., 2005. Induced chemical defenses in conifers: biochemical and molecular approaches to studying their function. In: Romeo, J.T. (Ed.), Chemical Ecology and Phytochemistry of Forest Ecosystems, Recent Advances in Phytochemistry, vol. 39. Elsevier, Amsterdam, pp. 1–28.

Takaya, Y., Terashima, K., Ito, J., He, Y.H., Tateoka, M., Yamaguchi, N., Niwa, M., 2005. Biomimic transformation of resveratrol. Tetrahedron 61, 10285–10290.

Tanaka, T., Iliya, I., Ito, T., Furusawa, M., Nakaya, K., Iinuma, M., Shirataki, Y., Matsuura, N., Ubukata, M., Murata, J., Simozono, F., Hirai, K., 2001. Stilbenoids in lianas of *Gnetum parvifolium*. Chem. Pharm. Bull. 49, 858–862.

Tao, J.M., Perdew, J.P., Staroverov, V.N., Scuseria, G.E., 2003. Climbing the density functional ladder: nonempirical meta-generalized gradient approximation designed for molecules and solids. Phys. Rev. Lett. 91, Art. No. 146401.

Tisler, V., Muck, T., 1999. Inks based on polystilbene spruce bark extract. Adv. Color Sci. Technol. 2, 191–196.

Viiri, H., Annila, E., Kitunen, V., Niemela, P., 2001. Induced responses in stilbenes and terpenes in fertilized Norway spruce after inoculation with blue-stain fungus, *Ceratocystis polonica*. Trees (Berlin, Germany) 15, 112–122.

Waffo-Teguo, P., Lee, D., Cuendet, M., Merillon, J.M., Pezzuto, J.M., Kinghorn, A.D., 2001. Two new stilbene dimer glucosides from grape (*Vitis vinifera*) cell cultures. J. Nat. Prod. 64, 136–138.

Weigend, F., Ahlrichs, R., 2005. Balanced basis sets of split valence, triple zeta valence and quadruple zeta valence quality for H to Rn: design and assessment of accuracy. Phys. Chem. Chem. Phys. 7, 3297–3305.

Xiang, T., Uno, T., Ogino, F., Ai, C.Q., Duo, J., Sankawa, U., 2005. Antioxidant constituents of *Caragana tibetica*. Chem. Pharm. Bull. 53, 1204–1206.

Yang, G.X., Zhou, I.T., Li, Y.Z., Hu, C.Q., 2005. Anti-HIV bioactive stilbene dimers of *Caragana rosea*. Planta Med. 71, 569–571.

Zeneli, G., Krokene, P., Christiansen, E., Krekling, T., Gershenzon, J., 2006. Methyl jasmonate treatment of mature Norway spruce (*Picea abies*) trees increases the accumulation of terpenoid resin components and protects against infection by *Ceratocystis polonica*, a bark beetle-associated fungus. Tree Physiol. 26, 977–988.